



Application of novel promising low-cost biosorbents in removing cationic and anionic dyes

Ibtissem Moussa^{a,b,*}, Manel Ben Ticha^{a,b}

^aUniversity of Monastir, Faculty of Sciences, UR13 ES 63 - Research Unity of Applied Chemistry & Environment, 5000 Monastir, Tunisia, Tel. +216 94892165; email: moussa.ibtissem@hotmail.fr (I. Moussa)

^bUniversity of Monastir, National Engineering School of Monastir, 5019 Monastir, Tunisia

Received 8 August 2018; 2 January 2019

ABSTRACT

Elimination of dyes in water resources must be averted and for that different treatment technologies are implicated. Among several methods, adsorption has an important place in dye removal. The increasing demand for low-cost and efficient treatment methods has given rise to inexpensive alternative adsorbents. In the present study, almond shells, almond stems, and fig stems were used as a new nonconventional and low-cost biosorbents for cationic and anionic dye adsorption in a batch process at 25°C. The adsorption characteristics of *Prunus amygdalus* and *Ficus carica* by-products were studied with respect to the variation in initial pH of dye solutions, biosorbent dosage, contact time, initial dye concentration, and salt concentration. The adsorption kinetics was analyzed using pseudo-first-order and pseudo-second-order models. The kinetic data were best described by the pseudo-second-order model. The equilibrium behavior of Basic Red 46 and Acid Blue 25 adsorption were examined by the Langmuir, Freundlich, Koble-Corrigan, and Redlich-Peterson isotherm models. It was found that the equilibrium data fitted well with the Langmuir model. The results revealed that the almond shells, almond stems, and fig stems could be used as low-cost alternative biosorbents for textile wastewater treatment.

Keywords: Biosorption; Acid Blue 25; Basic Red 46; Almond shell; Almond stem; Fig stem

1. Introduction

In the 21st century, environmental pollution is one of the major threats to human life. Wastewater is one of the major problems of pollution due to a wide quantity of water used in our quotidian life. Wastewater containing dye is the main source of water pollution. About 10,000 dyes are commercially available, and annual production of dyes is more than 7×10^5 metric tons worldwide. Dyes are widely used as coloring agents in great number of industries such as leather, cosmetic, plastic, food, textile, and pharmaceutical. Among these different industries, textile is the first in use of dyes for coloration of fiber. Thus, they generate an important quantity of colored wastewater. The existence of dyes in water, even at

small concentrations, is very apparent and undesirable. The complex aromatic structures make the dyes more stable to heat, oxidizing agents, and light and are generally biologically nondegradable. Besides, many dyes or their metabolites have carcinogenic, teratogenic, and mutagenic effects on humans and other life forms. Thus, it is important to eliminate dyes from wastewater before it is rejected.

In recent years, various methods such as ion exchange, coagulation, flocculation, advanced oxidation, and membrane separation have been reported and tested for the elimination of dyes from effluents. Most of these techniques are effective for the elimination of dyes. However, they are expensive and conduct to formation of sludge or by-products. Thus, the evolution of efficient, low-cost, and environmental-friendly technologies to reduce the quantity of dyes in wastewater

* Corresponding author.

is extremely necessary. Among treatment technologies, adsorption is quickly gaining importance. Commercial activated carbon is a very effective sorbent, but its high cost has limited its commercial application. In the recent years, the evolution of biosorption technology is a strong alternative for the removal of dyes from wastewaters with the benefits of greater profitability and efficiency, facility of process, and low cost. In recent decades, there has been a raise in the use of plant waste products for dye removal by biosorption from wastewater. Some examples of these low-cost alternative adsorbents are princess tree leaf [1], *Azolla pinnata* [2], soya bean [2], raw beech sawdust [3], maize cob [4], citrus peel [4], rice husk [4], and Barbary fig [5]. Nevertheless, the adsorption capacities of most of the above were still limited. New available, economical, and very effective biosorbents are still under evolution.

Almond shells, almond stems, and fig stems are in high quantity, cheap, and available in many regions of Tunisia. Tunisia ranked the 8th place in producing almond by about 3.8%. Indeed, Tunisia's annual production of almond shell is about 36,000 t as the shell has approximately 60% of the almond fruit weight [6]. The fig tree is a very widespread tree in Tunisia, and it grows in cold and humid as well as in hot and dry regions. These *Prunus amygdalus* and *Ficus carica* by-products have no commercial usage. There are no precedent published reports on the valorization of these agricultural wastes for removing dyes from aqueous solution. In this study, Basic Red 46 and Acid Blue 25 were selected as model synthetic dyes because of their several applications in textile industry. According to larger utilization of these dyes, high quantities of colored wastewater are ejected into environmental water sources. The discharge of these dyes into the environment is worrying because of their mutagenic, carcinogenic, and toxic characteristics. Therefore, elimination of these dyes from wastewater is an essential environmental problem. The main object of this research was to evaluate the feasibility of using the almond shells, almond stems, and fig stems as new nonconventional and low-cost adsorbents for the removal of Basic Red 46 and Acid Blue 25 from the aqueous solution. The effects of various parameters containing solution pH, biosorbent dosage, dye

concentration, and ionic strength were studied to optimize the biosorption process. Moreover, the kinetic and isotherm parameters were used to describe the experimental data.

2. Materials and methods

2.1. Preparation of biosorbent material

The almond shells, almond stems, and fig stems used in this work were collected in August 2014 from Monastir (a city on the central coast of Tunisia). They were washed with distilled water to remove soil and dust. After this, they were dried in natural conditions in September 2014. Then, the resultant biosorbents were grinded and sieved to a granulometry between 200 and 400 μm [6]. No other physical or chemical preparations were used before adsorption experiments.

2.2. Preparation of dye solution

Basic Red 46 and Acid Blue 25 were provided by a local textile factory. The structure of the dyes and their properties are given in Table 1 [2]. The dye stock solution of 500 mg L^{-1} was prepared by dissolving a quantity of dye powder in distilled water. The experimental solutions were prepared by diluting the dye stock solution to the desired concentration ranging from 10 to 800 mg L^{-1} . The pH of the solutions was adjusted with dilute NaOH (0.1 M) or HCl (0.1 M). All dye materials were used as supplied and without further purification.

2.3. Batch biosorption experiments

Adsorption experiments were carried out in a rotary shaker at 150 rpm and 25°C using 100-mL conical flasks containing 25 mL Basic Red 46 or Acid Blue 25 solutions in a water bath to elucidate the optimum values of the experimental parameters including solution pH (2–12), biosorbent dose (0.25–10 g L^{-1}), dye concentration (10–800 mg L^{-1}), and contact time (0–240 min). After each biosorption study, the samples were centrifuged (4,000 rpm, 10 min) for solid–liquid separation and the residual dye

Table 1
Properties of Basic Red 46 and Acid Blue 25

Dye properties	Basic Red 46	Acid Blue 25
Type	Cationic	Anionic
λ_{max} (nm)	532	602
M_w (g mol^{-1})	322	416
Structures		

concentration in solution was analyzed by an ultraviolet visible spectrophotometer (GBC, Cintra 202, Australia) at 530 and 602 nm for Basic Red 46 and Acid Blue 25, respectively. The equilibrium and kinetic studies were executed by defining optimum adsorption conditions. The quantity of adsorption, q_e (mg g^{-1}), was calculated by Eq. (1).

$$q_e = \frac{(C_0 - C_e)V}{m} \quad (1)$$

where C_0 and C_e are the initial and equilibrium concentrations of dye (mg L^{-1}), respectively; V is the volume of the solution (L); and m is the mass of dry biosorbent used (g).

The dye removal percentage can be calculated as Eq. (2).

$$\text{Removal percentage} = \frac{C_0 - C_e}{C_0} \times 100 \quad (2)$$

where C_0 and C_e (mg L^{-1}) are the liquid-phase concentrations of dye at initial and equilibrium, respectively.

The experiments were repeated, and the negative controls (without sorbent) were simultaneously carried out to make sure that adsorption was by biosorbents and not by the container.

2.4. Material characterization

2.4.1. Morphology

The surface morphologies of the adsorbent porosity were studied using a LEO scanning electron microscope (LEO-400) instrument.

2.4.2. Zero point of charge

The zero point of charge (pH_{ZPC}) pH of biosorbent materials were determined using the batch equilibrium technique with different weights (0.05, 0.1, 0.5, 1, 2.5, and 5 g) of raw material in 100 mL of NaCl solution of 0.1 mol L^{-1} . The initial pH value of the NaCl solution was adjusted ranging from 2 to 12 by adding 0.1 mol L^{-1} HCl or NaOH. The solutions were left to equilibrate in a magnetic stirrer for 24 h at $25^\circ\text{C} \pm 2^\circ\text{C}$. The pH values were measured again.

2.4.3. Conductometric titration

Before titration, the sample (0.6–1 g in 300 mL of deionized water) was acidified by adding 1 mL of HCl solution (0.1 mol L^{-1}) and extensively washed. The conductivity of the suspension material was then adjusted to $600 \mu\text{S cm}^{-1}$ with a 0.5 mol L^{-1} NaCl solution. Finally, the titration of 500 mL of a tested sample was performed with NaOH solution (0.01 mol L^{-1}), after the addition of 0.5 mL of a solution of HCl (0.1 mol L^{-1}).

2.4.4. Boehm titration

The Boehm titration method was determined to analyze the surface oxygen functional groups on activated carbon.

Before the titration, samples were dried for 3 h at 110°C . After this, the obtained samples (0.5 g) were added to bottles containing 25 mL of the following solutions (0.05 mol L^{-1}): NaOH, Na_2CO_3 , and NaHCO_3 . Then, the glass bottles were shaken for 48 h to attain equilibrium. The suspensions were filtered. Finally, the obtained filtrates (10 mL) were pipetted to 100 mL. The excess acid was back titrated with a NaOH solution (0.05 mol L^{-1}). The number of acidic sites was calculated assuming that NaHCO_3 neutralizes carboxylic groups; Na_2CO_3 neutralizes carboxylic and lactonic groups, while NaOH neutralizes carboxylic, phenolic, and lactonic groups.

2.4.5. Cation exchange capacity

The cation exchange capacity represents the minimum quantity of cations in milliequivalents that 1 g of material can exchange. One gram of the sample was added to glass bottle containing 100 mL of calcium. Once the exchange is done, the suspension was filtered. After dilution of the sample 100 times, 50 mL of this dilution is then titrated with a solution of ethylenediaminetetraacetic acid (EDTA) (0.02 N) in the presence of 2 mL of NaOH (2 mol L^{-1}) and a drop of Muroxide (colored indicator). The amount of residual calcium is then given by Eq. (3).

$$\text{Ca}_{\text{res}} \left(\frac{\text{meq}}{\text{L}} \right) = \frac{N_{\text{EDTA}} \times V_{\text{EDTA}}}{V_0} \times 1,000 \quad (3)$$

where N_{EDTA} is the normality of EDTA which is equal to 0.02 N, V_{EDTA} is the dosage volume (mL), and V_0 is the value of the test portion (mL).

The cation exchange capacity is then calculated according to Eq. (4).

$$\text{CEC} = \frac{\text{Ca}_0 - \text{Ca}_{\text{res}}}{m} \times V \quad (4)$$

where Ca_0 is the initial concentration of calcium (meq L^{-1}), Ca_{res} is the residual concentration of calcium (meq L^{-1}), m is the mass of the material (g), and V is the volume placed in contact with the material (L).

3. Results and discussion

3.1. Characterization of adsorbents

Fig. 1 shows SEM pictures of the adsorbents. An observation of the cross section showed strong presence of porous structure forming the cellular tissues of the material. These pores were very interesting for dye adsorption. The adsorption capacity of almond shells, almond stems, and fig stems depends upon porosity as well as chemical reactivity of functional groups at the surface. Knowing about surface functional groups would provide an idea of the adsorption capability of the adsorbents.

Table 2 summarizes the results of Boehm titration, cation exchange capacity, total charge, and pH_{ZPC} of the three adsorbents. The analysis of each biosorbent was investigated by the determination of acidic and basic groups using the

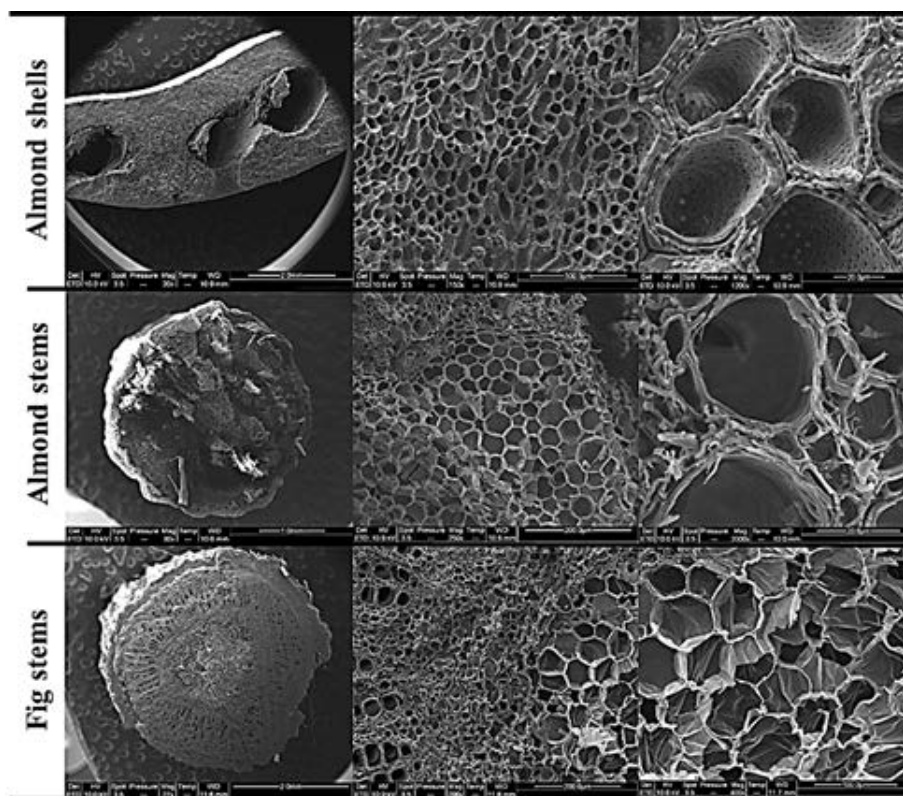


Fig. 1. SEM micrograph of the particles of the adsorbents.

Table 2
Boehm titration, cation exchange capacity, total charge, and pH_{ZPC} of biosorbents

	Almond shells	Almond stems	Fig stems
Carboxylic (10^{23} g^{-1})	0.265	0.308	0.631
Lactonic (10^{23} g^{-1})	0.032	0.017	0.019
Phenolic (10^{23} g^{-1})	1.166	1.144	0.843
Number of acidic sites (10^{23} g^{-1})	1.463	1.470	1.493
Number of basic sites (10^{23} g^{-1})	0.062	0.021	0.012
Cation exchange capacity (meq g^{-1})	6.24	5.6	8.08
Total charge ($\mu\text{eq g}^{-1}$)	65	80	110
pH_{ZPC}	4.65	6.4	6.75

Boehm titration. From Table 2, different conclusions were stated:

- the most of acidic functional groups are phenolic, followed by carboxylic and then lactonic;
- three adsorbents have an acid character leading to the great adsorption capacity of basic dyes;
- the fig stems presented the highest number of acidic sites and the lowest number of basic sites which confirms that this adsorbent possessed a higher affinity for basic dyes than the almond shells and stems;
- the almond shells had the highest number of basic sites which affirms that this adsorbent had a higher affinity for acidic dyes than the almond and fig stems.

Table 2 shows the isoelectric point of almond shells, almond stems, and fig stems. It is clear that these biosorbents are negatively charged in the range of $\text{pH} > \text{pH}_{\text{ZPC}}$ and positively charged in the range of $\text{pH} < \text{pH}_{\text{ZPC}}$.

3.2. Determination of optimum biosorption conditions

3.2.1. Effect of solution pH on dye adsorption

The pH of the aqueous solution is a significant parameter in the sorption of textile dyes. The effect of solution pH on Basic Red 46 and Acid Blue 25 sorption was studied at the pH ranges of 2–12, and the results are shown in Fig. 2. It is clear from the plots that the pH values for optimum removal

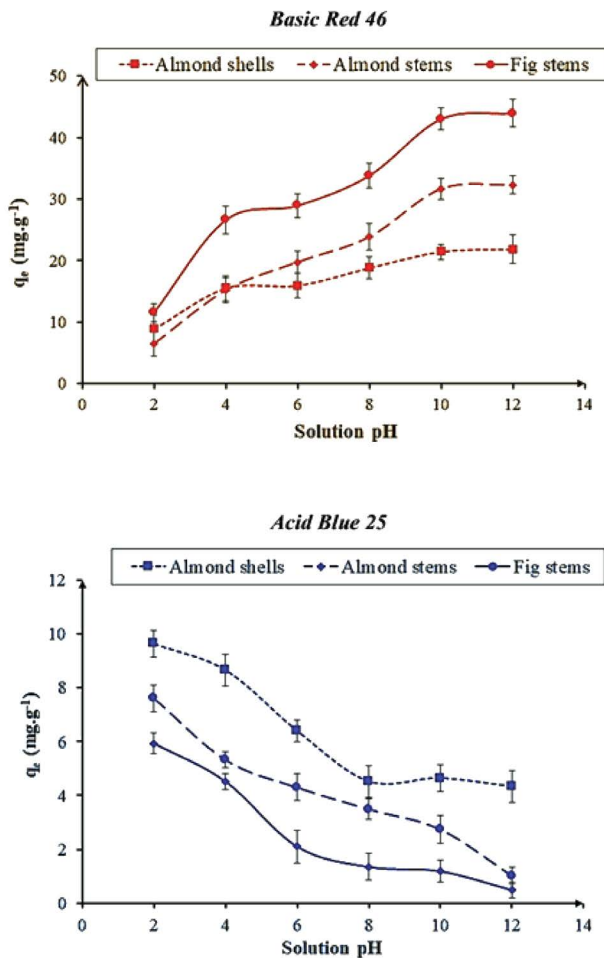


Fig. 2. Effect of pH on Basic Red 46 and Acid Blue 25 adsorption by almond shells, almond stems, and fig stems (initial dye concentration of 50 mg L^{-1} , temperature of 25°C , biosorbent dose of 5 g L^{-1} , and stirring speed of 150 rpm).

is 12 for Basic Red 46 and 2 for Acid Blue 25. The variation of adsorption with pH can be clarified by considering the variance in the electrokinetic behavior of adsorbents and the structure of dyes. Also, above the pH_{ZPC} the surface charge of the adsorbent is negative, and under this pH, the surface charge becomes positive. When the pH of solution is decreased under isoelectric point, the positive charge density on the surface of adsorbents increases, resulting in higher uptake of acidic dyes. Therefore, all the following investigations for Acid Blue 25 were performed at pH equal to 2. When the pH is increased, there is an electrostatic repulsion between negatively charged adsorption sites and negatively charged dye anions resulting in a decrease in the dye adsorption. Thus, the uptake of positively charged Basic Red 46 would be high. Apparently, the higher the solution pH value, the more the negative charges on the adsorbent surface, the more attractive to cations the biosorbent surface. Hence, pH equal to 12 is good for adsorbing Basic Red 46. It is important to note that although adsorbent surface has a positive charge density $\text{pH} < \text{pH}_{\text{ZPC}}$, it significantly adsorbs Basic Red 46. This may be explained by the fact that at lower pH values, positively charged surface sites

of almond shells, almond stems, and fig stems can attract anions from solutions and that compared with adsorbent surface in solution positively charged density would be situated more on the dye molecules at low pH value causing lower adsorption.

3.2.2. Effect of biosorbent dose on dye adsorption

The mass of biosorbent was varied in the range of $0.25\text{--}10 \text{ g L}^{-1}$ for the removal of Basic Red 46 and Acid Blue 25 from aqueous solution by almond shells, almond stems, and fig stems by keeping all other parameters such as pH, initial dye concentration, solution volume, temperature, and stirring speed. The effect of biosorbent dose on Basic Red 46 and Acid Blue 25 biosorption is shown in Fig. 3. The removal percentage of Basic Red 46 and Acid Blue 25 increased with increasing biosorbent dose. This is because of the presence of more biosorption sites and increased surface area as the dose of biosorbent increased. However, the amount of Basic Red 46 and Acid Blue 25 adsorbed per unit mass of biosorbent decreases with increasing biosorbent dosage because of the concentration gradient between solute concentrations in the solution and on the biosorbent surface. Therefore, with increasing biosorbent dosage, the quantity of dye biosorbed by unit weight of biosorbent decreased, thus resulting in a decrease in biosorption capacity with an increase in biosorbent dose. Similar results were previously reported by other researchers [7].

3.2.3. Effect of initial dye concentration on dye adsorption

The initial adsorbate concentration gives a significant driving force to overcome all mass transfer resistances of dyes between the aqueous and solid phases. The effect of initial dye concentration on biosorption of the Basic Red 46 and Acid Blue 25 was investigated in the range of $10\text{--}800 \text{ mg L}^{-1}$. The results are given in Fig. 4. The initial dye concentration has a significant effect on the adsorption capacity. The dye adsorption capacity of the biosorbent was increased with an increase in the initial dye concentration. The initial concentration of the dye that allows for optimal adsorption is equal to 250 and 500 mg L^{-1} for Basic Red 46 and Acid Blue 25, respectively.

3.3. Adsorption kinetic study

The pseudo-first-order and pseudo-second-order kinetic equations were used to examine the mechanism of adsorption processes such as chemical reaction and mass transfer. The kinetic data were analyzed using Lagergren's pseudo-first-order kinetic model for the adsorption of solid/liquid systems [8]. It can be expressed as Eq. (5).

$$q_t = q_e \times (1 - e^{-k_1 t}) \quad (5)$$

where q_t is the amount of dye adsorbed (mg g^{-1}) at time t (min), q_e is the amount of dye sorbed (mg g^{-1}) at equilibrium, and k_1 is the pseudo-first-order rate constant of sorption (min^{-1}).

The pseudo-second-order kinetic model, which is suggested by Ho [9], is based on the hypothesis that the

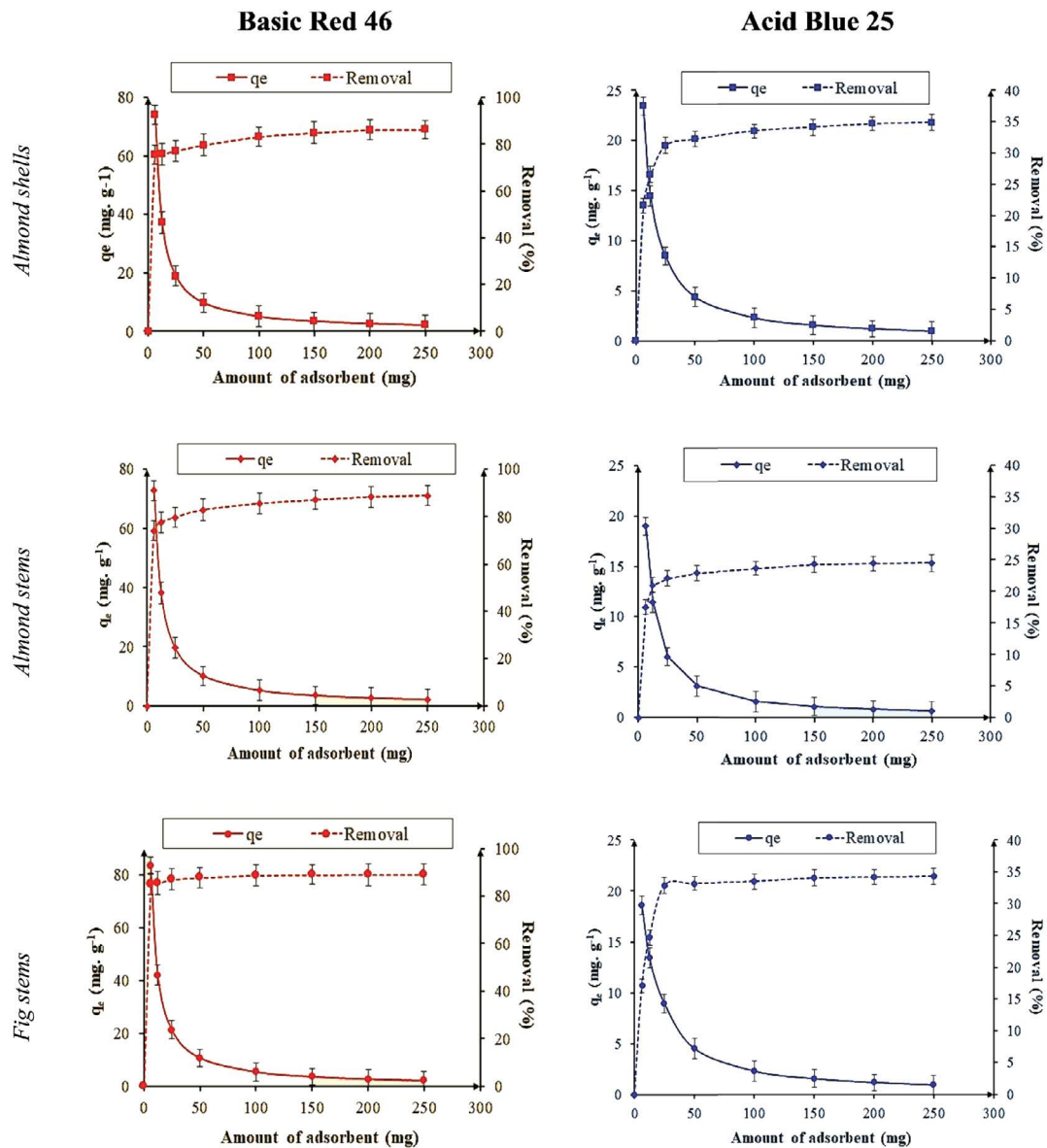


Fig. 3. Effect of biosorbent dose on Basic Red 46 (pH = 12) and Acid Blue 25 (pH = 2) adsorption by almond shells, almond stems, and fig stems (initial dye concentration of 50 mg L^{-1} , temperature of 25°C , and stirring speed of 150 rpm).

sorption follows second-order chemisorption. Its formula is given as Eq. (6).

$$q_t = \frac{q_e^2 k_2 t}{1 + (q_e k_2 t)} \quad (6)$$

where k_2 is the pseudo-second-order rate constant ($\text{g mg}^{-1} \text{min}^{-1}$).

Two kinetic models were tested to explain the data presented in Fig. 5: pseudo-first-order and pseudo-second-order models. The correlation coefficient (R^2) shows the agreement between model-calculated values and experimental data. The results are reported in Table 3. The lower values of R^2 and the difference between the experimental and calculated equilibrium sorption show that the

pseudo-first-order model failed to describe the adsorption kinetics. The higher values of $R^2 > 0.9$ and the good agreement between the experimental and calculated equilibrium sorption for the pseudo-second-order model affirm that this at last describes correctly the adsorption kinetics.

3.4. Adsorption equilibrium study

The capacity of the adsorption isotherm has an essential role in the determination of the maximum capacity of adsorption. It also indicates how efficiently an adsorbent will adsorb. The equilibrium relation between the concentrations of the adsorbate in the liquid phase and on the solid phase at a constant temperature is the adsorption isotherm. In the present investigation, equilibrium studies were carried out at optimum biosorption conditions. To adapt for the considered

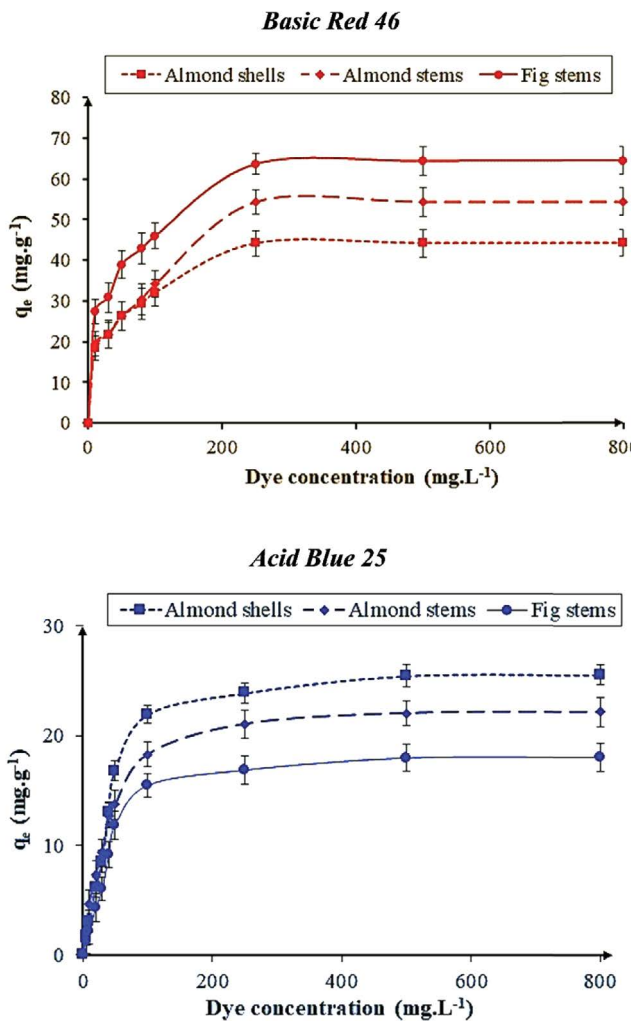


Fig. 4. Effect of initial dye concentration on Basic Red 46 (pH = 12 and biosorbent dose = 0.00625 g) and Acid Blue 25 (pH = 2 and biosorbent dose = 0.0125 g) adsorption by almond shells, almond stems, and fig stems.

system, a suitable model which can reproduce the experimental results obtained, equations of Langmuir, Freundlich, Redlich-Peterson and Koble-Corrigan have been considered.

Langmuir model is valid for monolayer coverage of adsorption of each molecule on a completely homogeneous surface. According to this model, when the sorbate occupies a site, further sorption cannot take place at that site. There is no interaction between molecules adsorbed on near sites, and all sites are energetically equivalent. The nonlinear equation of Langmuir isotherm model [10] is expressed as Eq. (7).

$$q_e = \frac{q_m K_L C_e}{1 + K_L C_e} \quad (7)$$

where C_e is the equilibrium dye concentration in the solution (mg L^{-1}), q_e is the amount of dye adsorbed on adsorbent at equilibrium (mg g^{-1}), q_m is the maximum adsorption capacity for the solid phase loading (mg g^{-1}), and K_L is the energy constant related to the heat of adsorption (L mg^{-1}).

The dimensionless constant separation factor for equilibrium parameter, R_L , which is one of essential characteristics of Langmuir model [11], is defined as Eq. (8).

$$R_L = \frac{1}{1 + K_L C_0} \quad (8)$$

where C_0 is the initial concentration of dye (mg L^{-1}).

The value of R_L indicates the type of isotherm to be irreversible ($R_L = 0$), favorable ($0 < R_L < 1$), linear ($R_L = 1$), or unfavorable ($R_L > 1$). For the present study, the R_L value indicates that the adsorption process of Basic Red 46 is favorable and the adsorption process of Acid Blue 25 is unfavorable.

Freundlich model applies to adsorption on heterogeneous surfaces. There is interaction between adsorbed molecules. According to this model, sorption energy exponentially decreases on completion of the sorption centers of a sorbent. Freundlich model [12] is expressed as Eq. (9).

$$q_e = K_f C_e^{1/n_f} \quad (9)$$

where K_f is the relative adsorption capacity of adsorbent (mg g^{-1}) (mg L^{-1}) $^{-1/n_f}$ and n_f is a constant related to adsorption intensity (dimensionless).

A value for $1/n_f$ under 1 shows a normal Langmuir isotherm, whereas $1/n_f$ above 1 indicates a cooperative adsorption [13].

The Redlich-Peterson isotherm [14] is a combination of Langmuir-Freundlich model. It is in accord with the high concentration of the Freundlich equation and approaches the Langmuir model at low concentration. The equation is given as Eq. (10).

$$q_e = \frac{K_R C_e}{1 + \alpha_R C_e^\beta} \quad (10)$$

where K_R is the Redlich-Peterson isotherm constant (L g^{-1}), α_R is the Redlich-Peterson isotherm constant (L mg^{-1}), and β is the exponent which lies between 0 and 1. The constant β can describe the isotherm as follows: if $\beta = 1$, the Langmuir will be the suitable isotherm, whereas if $\beta = 0$, the Freundlich isotherm will be the suitable isotherm.

Koble-Corrigan model [15] is another empirical model which is the combination of the Langmuir and Freundlich isotherm equations in one nonlinear equation for describing the equilibrium adsorption data. The equation is given as Eq. (11).

$$q_e = \frac{K_k C_e^\alpha}{1 + \alpha_k C_e^\alpha} \quad (11)$$

where K_k , α_k , and α are the Koble-Corrigan parameters.

The experimental data on the effect of an initial concentration of Basic Red 46 and Acid Blue 25 on the almond shells, almond stems, and fig stems of the test medium were fitted to the isotherm models using Origin 6.0, and the graphical representations of these models are presented in Fig. 5. All the constants are presented in Table 3. The value of R^2 closer to 1 shows that the respective equation better fits the

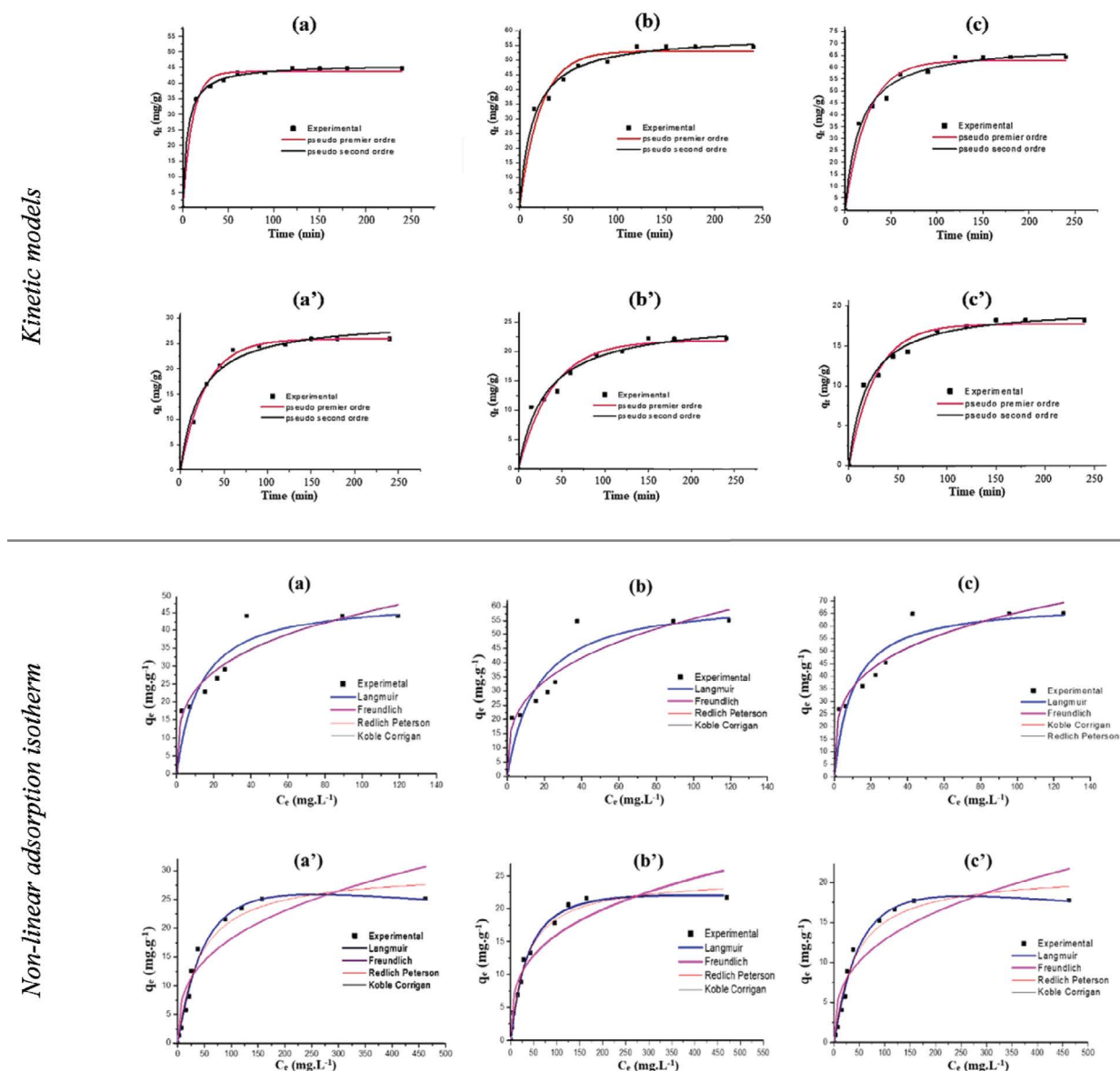


Fig. 5. Plots of kinetic models and nonlinear adsorption isotherm of Basic Red 46 and Acid Blue 25 onto almond shells ((a), (a')), almond stems ((b), (b')), and fig stems ((c), (c')) at 25°C.

experimental data. Based on the high correlation value, the Langmuir model represented best adsorption of Basic Red 46 and Acid Blue 25 onto the almond shells, almond stems, and fig stems.

3.5. Effect of ionic strength on dye adsorption

The effect of ionic strength on biosorption of Basic Red 46 and Acid Blue 25 by the almond shells, almond stems, and fig stems was analyzed in the sodium chloride solutions with concentrations ranging from 0.2 to 1.2 mol L⁻¹ for 120 and 150 min at the optimum biosorption conditions, respectively. As seen in Fig. 6, increasing the ion strength of solution caused an increase in sorption potential of Basic Red 46 and Acid Blue 25. This could be attributed to the fact that the salts favor the approximation association of the particles by

the formation of new surface sites where the dye molecules would be trapped. An increase in ionic strength has been shown to suppress electrostatic repulsion. The influence of salt concentration on basic dye adsorption is more important than the acid dye.

3.6. Comparison with other adsorbents

The application of available and inexpensive materials in wastewater treatment has been widely studied during recent years. Particularly, the Basic Red 46 and the Acid Blue 25 adsorption on different materials has been widely studied during recent years. In order to situate our natural adsorbent among those used to remove Basic Red 46 and Acid Blue 25 from aqueous solutions, a comparison based on maximum sorption capacity (q_m) was made. The results, illustrated in

Table 3

Kinetic parameters and adsorption isotherm constants for the adsorption of Basic Red 46 and Acid Blue 25 onto almond shells, almond stems, and fig stems at 25°C

Kinetic parameters												
Biosorbents	Basic Red 46						Acid Blue 25					
	Pseudo-first-order			Pseudo-second-order			Pseudo-first-order			Pseudo-second-order		
	q_e (mg g ⁻¹)	k_1 (min ⁻¹)	R^2	q_e (mg g ⁻¹)	k_2 (mg g ⁻¹ min ⁻¹)	R^2	q_e (mg g ⁻¹)	k_1 (min ⁻¹)	R^2	q_e (mg g ⁻¹)	k_2 (mg g ⁻¹ min ⁻¹)	R^2
Almond shells	53.088	0.045	0.886	55.523	15.40	0.970	25.855	0.06	0.879	26.581	8.034	0.977
Almond stems	53.691	0.050	0.878	55.529	16.89	0.982	21.719	0.007	0.766	25.165	6.025	0.954
Fig stems	62.817	0.052	0.888	65.970	17.88	0.998	18.509	0.0013	0.753	18.899	3.016	0.930

Adsorption isotherm constants														
Basic Red 46														
Biosorbents	Langmuir			Freundlich			Koble-Corrigan				Redlich-Peterson			
	q_m (mg g ⁻¹)	K_L (L mg ⁻¹)	R^2	K_f (mg g ⁻¹) $(\text{mg L}^{-1})^{-1/n}$	n_f	R^2	K_k	α_k	α	R^2	K_R	α_R	β	R^2
Almond shells	44.682	0.066	0.956	9.286	0.320	0.884	1.213	0.120	0.634	0.880	4.654	0.456	0.091	0.841
Almond stems	55.782	0.076	0.978	12.161	0.363	0.893	1.431	0.145	0.689	0.897	5.432	0.543	0.199	0.867
Fig stems	65.842	0.085	0.989	19.543	0.373	0.920	2.064	0.278	0.788	0.948	6.123	0.687	0.234	0.881

Acid Blue 25														
Biosorbents	Langmuir			Freundlich			Koble-Corrigan				Redlich-Peterson			
	q_m (mg g ⁻¹)	K_L (L mg ⁻¹)	R^2	K_f (mg ^{n-1/n}) $\text{L}^{1/n} \text{g}^{-1}$	n_f	R^2	K_k	α_k	α	R^2	K_R	α_R	β	R^2
Almond shells	26.182	7.858	0.895	0.028	0.341	0.784	1.185	0.03	0.699	0.750	6.671	0.465	0.899	0.770
Almond stems	25.139	7.451	0.881	0.018	0.320	0.79	1.102	0.004	0.529	0.748	5.768	0.357	0.691	0.756
Fig stems	17.646	5.330	0.789	0.004	0.311	0.746	0.764	0.005	0.310	0.765	2.908	0.234	0.677	0.728

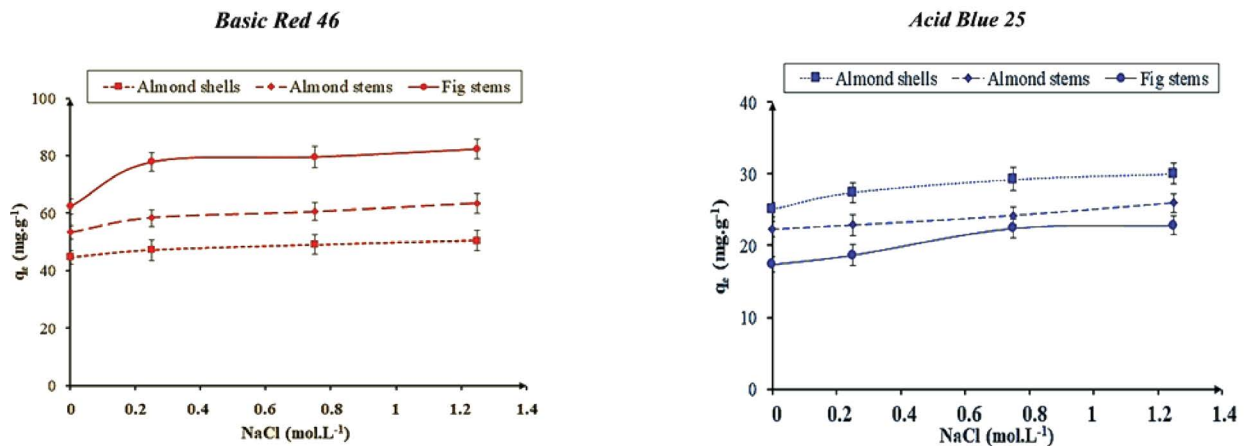


Fig. 6. Effect of ionic strength on Basic Red 46 (pH = 12, biosorbent dose = 0.00625 g, and initial dye concentration = 250 mg L⁻¹) and Acid Blue 25 (pH = 2, biosorbent dose = 0.0125 g, and initial dye concentration = 500 mg L⁻¹) adsorption by almond shells, almond stems, and fig stems.

Table 4
Comparison of almond shells, almond stems, and fig stems with other sorbents for Basic Red 46 and Acid Blue 25 sorption

Adsorbates	Adsorbents	q_m (mg g ⁻¹)	References
Basic Red 46	Boron industry waste	74.73	[17]
	Fir sawdust	20.47	[18]
	Beech sawdust	19.24	[18]
	Crud clay	54	[16]
	Princess tree leaf	43.1	[1]
	Gypsum	39.17	[19]
	Rice husk	40.50	[19]
	Raw beech sawdust	9.78	[3]
	Jute processing waste	22.47	[20]
	Almond shells	44.68	Present study
	Almond stems	55.78	Present study
Fig stems	65.84	Present study	
Acid Blue 25	Wood sawdust (raw)	5.92	[21]
	Peat	12.7	[23]
	Hazelnut shell	60.2	[22]
	Saw dust-walnut	36.98	[22]
	Saw dust-cherry	31.98	[22]
	Saw dust-oak	27.85	[22]
	Saw dust-pitch pine	26.19	[22]
	Bagasse pith (raw)	17.5	[23]
	Wood	7.0–11.6	[22]
	Almond shells	26.18	Present study
	Almond stems	25.14	Present study
Fig stems	17.65	Present study	

Table 4, had shown that the almond shells, almond stems, and fig stems could be considered as a promising material to remove Basic Red 46 and Acid Blue 25 when compared with the common natural mineral and lignocellulosic materials. The adsorption capacity of Basic Red 46 onto almond shells, almond stems, and fig stems is higher than mineral materials such as crud clay [16] and lower than boron industry waste [17]. In comparison with other lignocellulosic materials, the adsorption capacity of Basic Red 46 onto our biosorbents is higher than fir sawdust [18], beech sawdust [18], princess tree leaf [1], rice husk [19], raw beech sawdust [3], and Jute processing waste [20]. On the other hand, the adsorption capacity of Acid Blue 25 onto almond shells, almond stems, and fig stems is higher than other lignocellulosic materials such as wood sawdust [21], wood [22], and bagasse pith [23]. Thus, almond shells, almond stems, and fig stems could be considered among the most efficient natural material for the removal of Acid Blue 25 and especially Basic Red 46.

4. Conclusions

The results reported herein indicate that almond shells, almond stems, and fig stems could be successfully used to remove Basic Red 46 and Acid Blue 25 from aqueous solution by sorption process. The regeneration of the saturated biosorbent materials with Basic Red 46 or Acid

Blue 25 does not require while the building reuse is possible. Thus, desorption and recovery processes could be avoided and the related costs reduced. Consequently, for environmental, economic, and operational considerations, the use of almond shells, almond stems and fig stems for the removal of Basic Red 46 or Acid Blue 25 and other nutrients appears to be more promising.

Acknowledgments

The authors gratefully express their sincere gratitude to Prof. Dr. Mohamed Naceur Belgacem (Director of Pagora-INP Grenoble, France) as well as Dr. Bertine Khélifi (LGP2, INP Grenoble), for her help and availability.

References

- [1] F. Deniz, S.D. Saygideger, Removal of a hazardous azo dye (Basic Red 46) from aqueous solution by princess tree leaf, *Desalination*, 268 (2011) 6–11.
- [2] M.R.R. Kooch, M.K. Dahri, L.B.L. Lim, L.H. Lim, Batch adsorption studies on the removal of acid blue 25 from aqueous solution using *Azolla pinnata* and soya bean waste, *Arabian J. Sci. Eng.*, 41 (2016) 2453–2464.
- [3] F.A. Batzias, D.K. Sidiras, Dye adsorption by prehydrolysed beech sawdust in batch and fixed-bed systems, *Bioresour. Technol.*, 98 (2007) 1208–1217.
- [4] S. Saroj, S.V. Singh, D. Mohan, Removal of colour (Direct Blue 199) from carpet industry wastewater using different biosorbents (maize cob, citrus peel and rice husk), *Arabian J. Sci. Eng.*, 40 (2015) 1553–1564.
- [5] A. Seghier, M. Hadjel, N. Benderdouche, Adsorption study of heavy metal and acid dye on an amphoteric biomaterial using barbary fig skin, *Arabian J. Sci. Eng.*, 42 (2017) 1487–1496.
- [6] I. Moussa, N. Baaka, R. Khiari, A. Moussa, G. Mortha, M.F. Mhenni, Application of *Prunus amygdalus* by-products in eco-friendly dyeing of textile fabrics, *J. Renewable Mater.*, 6 (2018) 55–67.
- [7] H. Saygılı, F. Güzel, Behavior of mesoporous activated carbon used as a remover in Congo red adsorption process, *Water Sci. Technol.*, 2017 (2018) 170–183.
- [8] S. Lagergren, About the theory of so-called adsorption of soluble substances, *K. Sven. Vetensk.akad. Handl.*, 24 (1898) 1–39.
- [9] Y. Ho, G. McKay, Pseudo-second-order model for sorption processes, *Process Biochem.*, 34 (1999) 451–465.
- [10] I. Langmuir, The adsorption of gases on plane surfaces of glass, mica and platinum, *J. Am. Chem. Soc.*, 40 (1918) 1361–1403.
- [11] S.V. Mohan, N.C. Rao, J. Karthikeyan, Adsorptive removal of direct azo dye from aqueous phase onto coal based sorbents: a kinetic and mechanistic study, *J. Hazard. Mater.*, 90 (2002) 189–204.
- [12] H.M.F. Freundlich, Over the adsorption in solution, *Z. Phys. Chem.*, 57 (1906) 385–470.
- [13] B.H. Hameed, A.T.M. Din, A.L. Ahmad, Adsorption of methylene blue onto bamboo-based activated carbon: kinetics and equilibrium studies, *J. Hazard. Mater.*, 141 (2007) 819–825.
- [14] O. Redlich, D.L. Peterson, A useful adsorption isotherm, *J. Phys. Chem.*, 63 (1959) 1024–1024.
- [15] R.A. Koble, T.E. Corrigan, Adsorption isotherms for pure hydrocarbons, *Ind. Eng. Chem.*, 44 (1952) 383–387.
- [16] A.B. Karim, B. Mounir, M. Hachkar, M. Bakasse, A. Yaacoubi, Removal of Basic Red 46 dye from aqueous solution by adsorption onto Moroccan clay, *J. Hazard. Mater.*, 168 (2009) 304–309.
- [17] A. Olgun, N. Atar, Equilibrium and kinetic adsorption study of Basic Yellow 28 and Basic Red 46 by a boron industry waste, *J. Hazard. Mater.*, 161 (2009) 148–156.

- [18] L. Laasri, M.K. Elamrani, O. Cherkaoui, Removal of two cationic dyes from a textile effluent by filtration-adsorption on wood sawdust, *Environ. Sci. Pollut. Res. Int.*, 14 (2007) 237–240.
- [19] V. Vadivelan, K.V. Kumar, Equilibrium, kinetics, mechanism, and process design for the sorption of methylene blue onto rice husk, *J. Colloid Interface Sci.*, 286 (2005) 90–100.
- [20] S. Banerjee, M.G. Dastidar, Use of jute processing wastes for treatment of wastewater contaminated with dye and other organics, *Bioresour. Technol.*, 96 (2005) 1919–1928.
- [21] Y.S. Ho, G. McKay, Kinetic models for the sorption of dye from aqueous solution by wood, *Process Saf. Environ. Prot.*, 76 (1998) 183–191.
- [22] V.J.P. Poots, G. McKay, J.J. Healy, The removal of acid dye from effluent using natural adsorbents—II Wood, *Water Res.*, 10 (1976) 1067–1070.
- [23] B. Chen, C.W. Hui, G. McKay, Film-pore diffusion modeling and contact time optimization for the adsorption of dyestuffs on pith, *Chem. Eng. J.*, 84 (2001) 77–94.